Biochemistry and Biophysics Reports 29 (2022) 101207

Contents lists available at ScienceDirect

Biochemistry and Biophysics Reports

journal homepage: www.elsevier.com/locate/bbrep

Ingestion of hemozoin by peripheral blood mononuclear cells alters temporal gene expression of ubiquitination processes

Samuel B. Anyona [a,b,*], Qiuying Cheng [c], Evans Raballah [b,d], Ivy Hurwitz [c], Christophe G. Lambert [c], Benjamin H. McMahon [e], Collins Ouma [b,f], Douglas J. Perkins [b,c]

[a] Department of Medical Biochemistry, School of Medicine, Maseno University, Maseno, 40105, Kenya
[b] University of New Mexico-Kenya Global Health Programs, Kisumu and Siaya, 40100, Kenya
[c] Center for Global Health, University of New Mexico, Albuquerque, NM, 87131, United States
[d] Department of Medical Laboratory Sciences, School of Public Health, Biomedical Sciences and Technology, Masinde Muliro University of Science and Technology, Kakamega, 50100, Kenya
[e] Theoretical Biology and Biophysics Group, Theoretical Division, Los Alamos National Laboratory, Los Alamos, NM, 87544, United States
[f] Department of Biomedical Sciences and Technology, School of Public Health and Community Development, Maseno University, Maseno, 40105, Kenya

ARTICLE INFO

Keywords:
Ubiquitination
Gene expression
in vitro malaria model
Hemozoin
PBMCs

ABSTRACT

Plasmodium falciparum (Pf) malaria is among the leading causes of childhood morbidity and mortality worldwide. During a natural infection, ingestion of the malarial parasite product, hemozoin (*Pf*Hz), by circulating phagocytic cells induces dysregulation in innate immunity and enhances malaria pathogenesis. Treatment of cultured peripheral blood mononuclear cells (PBMCs) from healthy, malaria-naïve donors with physiological concentrations of *Pf*Hz can serve as an *in vitro* model to investigate cellular processes. Although disruptions in host ubiquitination processes are central to the pathogenesis of many diseases, this system remains unexplored in malaria. As such, we investigated the impact of *Pf*Hz on the temporal expression patterns of 84 genes involved in ubiquitination processes. Donor PBMCs were cultured in the absence or presence of *Pf*Hz for 3-, 9-, and 24 h. Stimulation with *Pf*Hz for 3 h did not significantly alter gene expression. Incubation for 9 h, however, elicited significant changes for 6 genes: 4 were down-regulated (*FBXO4*, *NEDD8*, *UBE2E3,* and *UBE2W*) and 2 were up-regulated (*HERC5* and *UBE2J1*). *Pf*Hz treatment for 24 h significantly altered expression for 14 genes: 12 were down-regulated (*ANAPC11*, *BRCC3*, *CUL4B*, *FBXO4*, *MIB1*, *SKP2*, *TP53*, *UBA2*, *UBA3*, *UBE2G1*, *UBE2G2*, and *WWP1*), while 2 were up-regulated (*UBE2J1* and *UBE2Z*). Collectively, these results demonstrate that phagocytosis of *Pf*Hz by PBMCs elicits temporal changes in the transcriptional profiles of genes central to host ubiquitination processes. Results presented here suggest that disruptions in ubiquitination may be a previously undiscovered feature of malaria pathogenesis.

1. Introduction

Malaria continues to pose a global health challenge, with an estimated 229 million infections reported worldwide in 2019, 94% of which occur in the World Health Organization (WHO) African region [1]. Malaria control efforts include the use of Artemisinin Combination Therapy for case management, and distribution of long-lasting impregnated nets and indoor residual spraying for vector control. Despite progress, these gains are threatened by the emergence of parasite resistance to antimalarial drugs, vector resistance to insecticides, and parasite deletions on the *pf*hrp2 and *pf*hrp3 (*pf*hrp2/3) genes used for monitoring [1]. With globally persistent morbidities and mortalities among children (<5 years of age) and pregnant women, largely in moderate and high *Plasmodium falciparum* transmission regions of sub-Saharan Africa [1], there is need for studies on the cellular processes underlying the etiology of malaria pathogenesis.

Immune responses to malaria infection in the human host include, among others, parasitic products and antigens that trigger innate and cellular pathways [2]. Previous studies have shown an association between malarial pigment (hemozoin) containing monocytes and inhibition of the erythropoietic cascade in children with malarial anemia [3,4]. In *P. falciparum* infections, formation of hemozoin occurs during the asexual replication cycle where metabolism of host hemoglobin by the parasites leaves the iron-rich, toxic ferriprotoporphyrin IX that

* Corresponding author. Department of Medical Biochemistry, School of Medicine, Maseno University, Maseno, 40105, Kenya.
E-mail address: sanyona@maseno.ac.ke (S.B. Anyona).

https://doi.org/10.1016/j.bbrep.2022.101207
Received 26 November 2021; Received in revised form 6 January 2022; Accepted 8 January 2022

aggregates to an insoluble pigment (reviewed in Ref. [5]). Accumulated *P. falciparum* hemozoin (*Pf*Hz) is ingested by host phagocytes, and serves as indirect markers of parasite sequestration, schizogony, and severe disease [6]. There is a wealth of information showing the relationship between host phagocytic ingestion of *Pf*Hz and inefficient erythropoiesis, decreased hematocrit, and severe disease [3,4,6–8]. As such, phagocytosis of *Pf*Hz in cultured peripheral blood mononuclear cells (PMBCs) can serve as a viable *in vitro model* to investigate the temporal dynamics of cellular processes that are not practical *in vivo* in humans.

Severe malaria is characterized by activation of the inflammatory cascade, a consequence of induction of the innate immune response, that triggers an array of pro- and anti-inflammatory cytokines, chemokines, and effector molecules [5]. During innate immune responses, the proteostasis network is influenced by the synthesis of pathogen proteins, inflammatory tissue damage caused by free radicals, and molecules released by phagocytes [9]. The ubiquitin proteasome system (UPS) is an intracellular lysosomal free pathway that plays a critical role in preserving proteostasis, as well as process antigen for presentation to the major histocompatibility (MHC) class I, proliferation of the cell cycle, and signaling mechanisms (reviewed in Ref. [10]).

The UPS is a complex mechanism, controlled by > 1000 genes (reviewed in Ref. [10]), which encode proteins and components that select and modify intracellular substrates for ubiquitination and subsequent degradation by proteasomes [11,12]. Ubiquitination is mediated by a cascade of events involving three enzymes: namely ubiquitin-activating enzyme (E1), ubiquitin-conjugating enzyme (E2), and ubiquitin ligases (E3). E1 forms a covalent bond between a cysteine residue on its active site and a C-terminal glycine of ubiquitin [13]. The activated ubiquitin molecule is transferred to E2, which then binds to E3, thus enabling recognition of specific targets [14]. Substrate specificity is mediated by ~500–1000 putative E3 ligases encoded by the human genome [15]. The tagged ubiquitinated proteins are presented to the proteasome for degradation, thereby ensuring preservation of homeostasis for the host and protection of cells from harmful protein aggregation that may compromise cell integrity and function [16].

Given the importance of the UPS for cellular functions, we hypothesized that ubiquitination may play a central role in the pathogenesis of malaria. The selection of the UPS was based on a global transcriptome profiling of clinical samples drawn from children presenting with malaria anemia in a rural hospital in western Kenya. The samples, which represented "polarized extremes" of clinical phenotypes were classified into non-severe malaria anemia [non-SMA, (Hb, 8.0–10.9 g/dL; avg. Hb = 9.4 g/dL), n = 35] and severe malarial anemia [SMA, (Hb, ≤5.0 g/dL; avg. Hb = 3.6 g/dL), n = 13]. Children with co-infections (HIV-1 and Bacteremia) and/or haemoglobinopathies (α^+-thalassemia deletions, glucose-6-phosphate dehydrogenase deficiency and sickle cell traits variants) were excluded from analysis. The Illumina® HumanHT-12 v4 beadchip (Illumina®, CA, USA), with N19,185 transcripts on the Illumina® "iScanSQ" platform was used to quantify global gene expression profiles in total RNA isolated from white blood cells. Differentially expressed genes between non-SMA and SMA were identified and used to generate relational networks using the web-based algorithm, MetaCore™ software suite (Clarivate Analytics, Philadelphia, PA, USA). Among the bio-molecular networks showing the highest significance ($P = 3.53 \times 10^{-19}$) was the signal transduction gene pathway mediated by ubiquitin. To better understand the role of ubiquitination processes in human malaria, we recently determined the transcriptional profiles of 84 key ubiquitination genes in Kenyan children who presented at hospital with either mild or severe malarial anemia. This investigation discovered differentially expressed genes (DEG) for ubiquitination processes in children with severe disease [17]. To extend this recent knowledge, the current study analyzed the temporal dynamics of the same set of genes using an *in vitro* model of malaria. Results presented here show that ingestion of *Pf*Hz induces temporal changes in the expression of genes central to ubiquitination.

2. Materials and methods

2.1. Preparation of P. falciparum hemozoin

Crude hemozoin used in the *in vitro* experiments was isolated from *P. falciparum* infected erythrocytes cultured in a mycoplasma-negative environment as described previously [3,18,19]. Briefly, a laboratory strain of *P. falciparum* (*Pf*.D6), was cultured in normal human O^+ erythrocytes obtained from fresh whole blood drawn from healthy donors. Parasite cultures were maintained *in vitro* using continuous culture conditions [20]. Cultures at an initial parasitemia of 2% were enriched for ring stages using D-sorbitol [21]. At >5% infectivity with late trophozoite and early schizont stages, parasite cultures were harvested and the erythrocyte pellet was lysed using 15% saponin in 0.01 M phosphate-buffered saline. Upon confirmation of complete lysis of erythrocytes by microscopy, pellets were washed, sonicated to remove lipids, and dried overnight at 40 °C on a heat block. Pellets were re-suspended in sterile water (1.0 mg/mL final concentration). Levels of endotoxin in the hemozoin prepared were quantified using the Limulus amebocyte lysate test (Thermo Fisher Scientific, Waltham, MA, USA) and quantities of <0.1 EU/mL recorded. With an estimation of 5.0 EU/mL being equivalent to 1.0 ng/mL of endotoxin, the final hemozoin preparation contained <0.02 ng/mL of endotoxin in the preparation.

2.2. In vitro isolation and culture of donor PBMCs

PBMCs from fresh whole blood donated by three healthy, malaria-naïve donors were separated using the Ficoll-Hypaque technique according to published methods, with minor modifications [3,8,22]. PBMCs (3.0×10^6 cells/mL), in triplicates, were seeded in 6-well plates at 37°C in 5% CO_2 atmosphere for 2 h in RPMI 1640 media. A set of triplicate PBMC cultures were treated with a physiological concentration of *P. falciparum* hemozoin [*Pf*Hz (10 μg/mL)] that mimics the concentration in children with severe malaria [18], along with controls under identical conditions without *Pf*Hz. Cultures were harvested at 3-, 9-, and 24-h intervals post-treatment, washed, lysed, and stored at −80°C until use.

2.3. Isolation of RNA and synthesis of complementary DNA (cDNA)

Total RNA from cultured PBMCs were isolated using the RNeasy Mini Kit (Qiagen, LLC-USA, Germantown, MD, USA), according to the manufacturer's instructions. RNA was further processed using the RNA Clean and Concentrator Kit (ZYMO Research Corp., Irvine, CA, USA). The quantity of RNA was measured using a NanoDrop 2000 Spectrophotometer (Thermo Fisher Scientific, Waltham, MA, USA). The quality and integrity of the purified RNA were estimated using an automated Agilent 2100 Bioanalyzer (Agilent Technologies, Santa Clara, CA, USA). Only samples with an RNA integrity number (RIN) ≥8 were used for cDNA synthesis.

cDNA was synthesized using the RT^2 First Strand Kit (Qiagen, LLC-USA, Germantown, MD, USA) in a 2-step procedure that involved genomic DNA elimination and reverse transcription, according to the manufacturers protocol. The RT^2 First Strand Kits used for the data presented were optimized for real-time PCR-based gene expression analysis using RT^2 Profiler PCR Arrays.

2.4. Determination of ubiquitination gene expression profiles

Human Ubiquitination Pathway RT^2 Profiler PCR Array kit (Qiagen, LLC-USA, Germantown, MD, USA) was used to measure mRNA transcript levels of 84 key ubiquitination process genes. To account for the quality and integrity of the resulting expression reads, the array kit incorporated 5 housekeeping gene controls [actin, beta (*ACTB*), beta-2-microglobulin (*B2M*), glyceraldehyde-3-phosphate dehydrogenase (*GAPDH*), hypoxanthine phosphoribosyl-transferase 1 (*HPRT1*), and

ribosomal protein, large, P0 (*RPLPO*)], along with 3 reverse transcription controls, 3 positive PCR controls, and 1 human genomic DNA contamination control. For each donor cDNA sample, reaction master mixes (equivalent for 96 wells) were prepared as per manufacturers' protocol, and contained, 1 × RT^2 SYBR Green mastermix, 0.5 μg cDNA synthesis mix, and RNase-free water. Aliquots (25 μL) of the assay mix were dispensed into 96-well RT^2 Profiler PCR Array plates (Qiagen, LLC-USA, Germantown, MD, USA). Each well of the RT^2 Profiler PCR Array contained a primer assay mixed with an inert dye for quality control. Amplification was performed on a StepOne Plus Real Time PCR system (Thermo Fisher Scientific, Waltham, MA, USA), at an initial denaturation temperature of 95°C for 10 min, followed by 40 cycles at 95°C for 15 s, and 60°C for 1 min. To test the specificity of the amplification, dissociation curve analysis was performed, with the ramp set from 60°C to 95°C.

2.5. Data analysis

The cycle threshold (C_T) value for each well was calculated using the Real-Time Cycler software (Thermo Fisher Scientific, Waltham, MA, USA). Baseline levels were defined by selecting the automated baseline option on the Real Time PCR thermocycler (Thermo Fisher Scientific, Waltham, MA, USA). The threshold was set manually by using the log view of the amplification plots, and data containing the C_T values were exported to a Microsoft Excel spreadsheet. The RT^2 Profiler PCR Array data was uploaded and analyzed using a web-based data analysis tool, the GeneGlobe Data Analysis Center (https://geneglobe.qiagen.com/us/analyze). Gene expression levels were determined using the $^{\Delta\Delta}C_T$ method, where fold change was calculated by converting the ΔC_T from a log2 scale to a linear scale. The $2^{-\Delta C_T}$ was determined for each gene on the ubiquitination process [23]. Upregulated gene expression is presented by values > 1, while downregulated gene expression is denoted by values between 0 and 1. To accurately infer biological relevance, fold regulation ($-1/x$) values are represented. *P*-values were calculated using the student's *t*-test (two-tail distribution and equal variances assumed) on the $2^{-\Delta\Delta C_T}$ values for each gene in the control (untreated) PMBCs relative to the *Pf*Hz treatment PBMCs at 3-, 9- and 24 h, with values $\leq$ 0.05 being considered statistically significant.

3. Results

3.1. Quantity and quality of RNA from cultured PBMCs following experimental manipulation

Following the isolation, culture and treatment of donor PBMCs, RNA from both control and treatments arms were isolated. To ensure that the integrity of RNA was maintained following experimental manipulation, both the quantity and quality were determined (Fig. 1). The RNA integrity number (RIN) for all samples was ≥8.0, ensuring appropriate quality for cDNA synthesis. The RNA quantity was adjusted to a uniform level of 0.5 μg for each sample before synthesis of cDNA. For measurement of mRNA transcripts, 0.5 μg of cDNA was used for each sample.

3.2. Impact of PfHz on temporal expression profiles of host ubiquitination genes

We determined the effect of crude *Pf*HZ on a set of 84 genes involved in the host ubiquitination process using an *in vitro* model of malaria. Treatment of cultured PBMCs using a physiological concentration of *Pf*Hz (10 μg/mL) for 3 h did not result in significant DEG for any of the 84 ubiquitination genes (Fig. 2A). However, *Pf*Hz stimulation for 9 h elicited significant differential regulation for 6 genes: 4 genes were down-regulated (*FBX04, NEDD8, UBE2E3, and UBE2W*), whereas 2 genes were up-regulated (*HERC5* and *UBE2J1*, Fig. 2B). In addition, *Pf*Hz treatment for 24 h resulted in significant changes in 14 genes: 12 genes were down-regulated (*ANAPC11, BRCC3, CUL4B, FBXO4, MIB1, SKP2, TP53, UBA2, UBA3, UBE2G1, UBE2G2*, and *WWP1*) and 2 genes were up-regulated (*UBE2J1* and *UBE2Z*, Fig. 2C).

The fold-regulation for differential gene expression between the control (non-stimulated) and stimulated (*Pf*Hz) PBMCs for 3, 6, and 24 h ranged from 3.8 to −2.6 (Fig. 2D). The non-supervised hierarchical cluster analysis for each of the donors at 3, 6, and 24 h is shown in Fig. 2E.

There was a difference of ≥1.5-fold regulation in *Pf*Hz-treated cells relative to the control group after 9 h for three genes (Table 1). Two genes were up-regulated: Hect domain and RLD 5 (*HERC5*; fold-regulation = 2.27, $P = 0.026$) and Ubiquitin-conjugating enzyme E2, J1, (*UBE2J1*; fold-regulation = 2.12, $P = 0.024$). In contrast, one gene was down-regulated at 9 h: Ubiquitin-conjugating enzyme E2E 3 (*UBE2E3*; fold-regulation = −1.55, $P = 0.010$).

Stimulation of PBMCs for 24 h with *Pf*Hz induced DEG at ≥1.5-fold

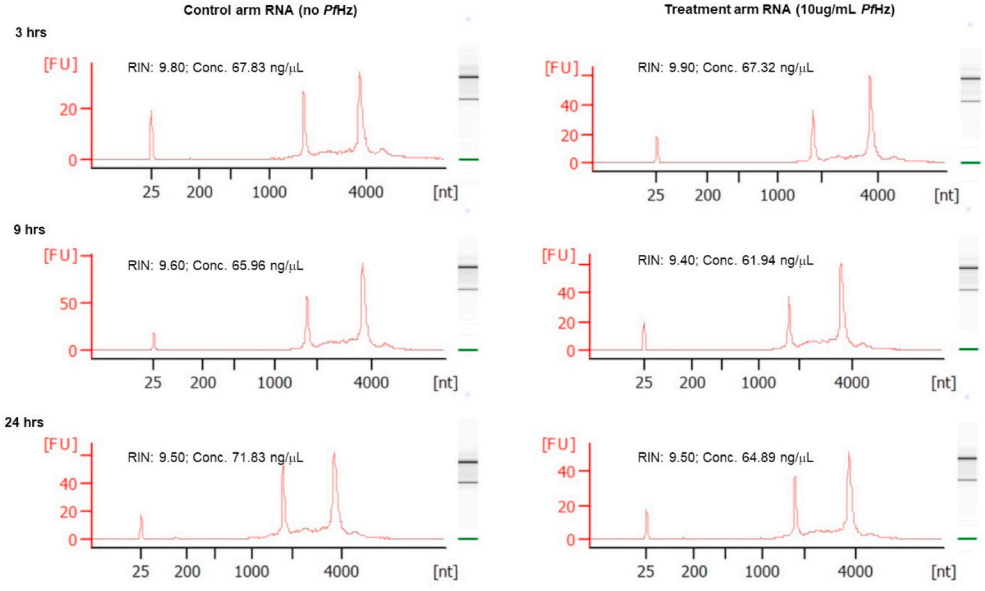

Fig. 1. RNA quality and quantity for cultured PBMCs. RNA from the cultured peripheral blood mononuclear cells (PBMCs) was isolated using the RNeasy Mini Kit (Qiagen, LLC-USA, Germantown, MD, USA). The quantity of RNA was measured using NanoDrop 2000 Spectrophotometer (Thermo Fisher Scientific, Waltham, MA, USA). The quality and integrity of the purified RNA were estimated using an automated Agilent 2100 Bioanalyzer (Agilent Technologies, Santa Clara, CA, USA). Samples with RNA integrity number (RIN) ≥8 were used for cDNA synthesis.

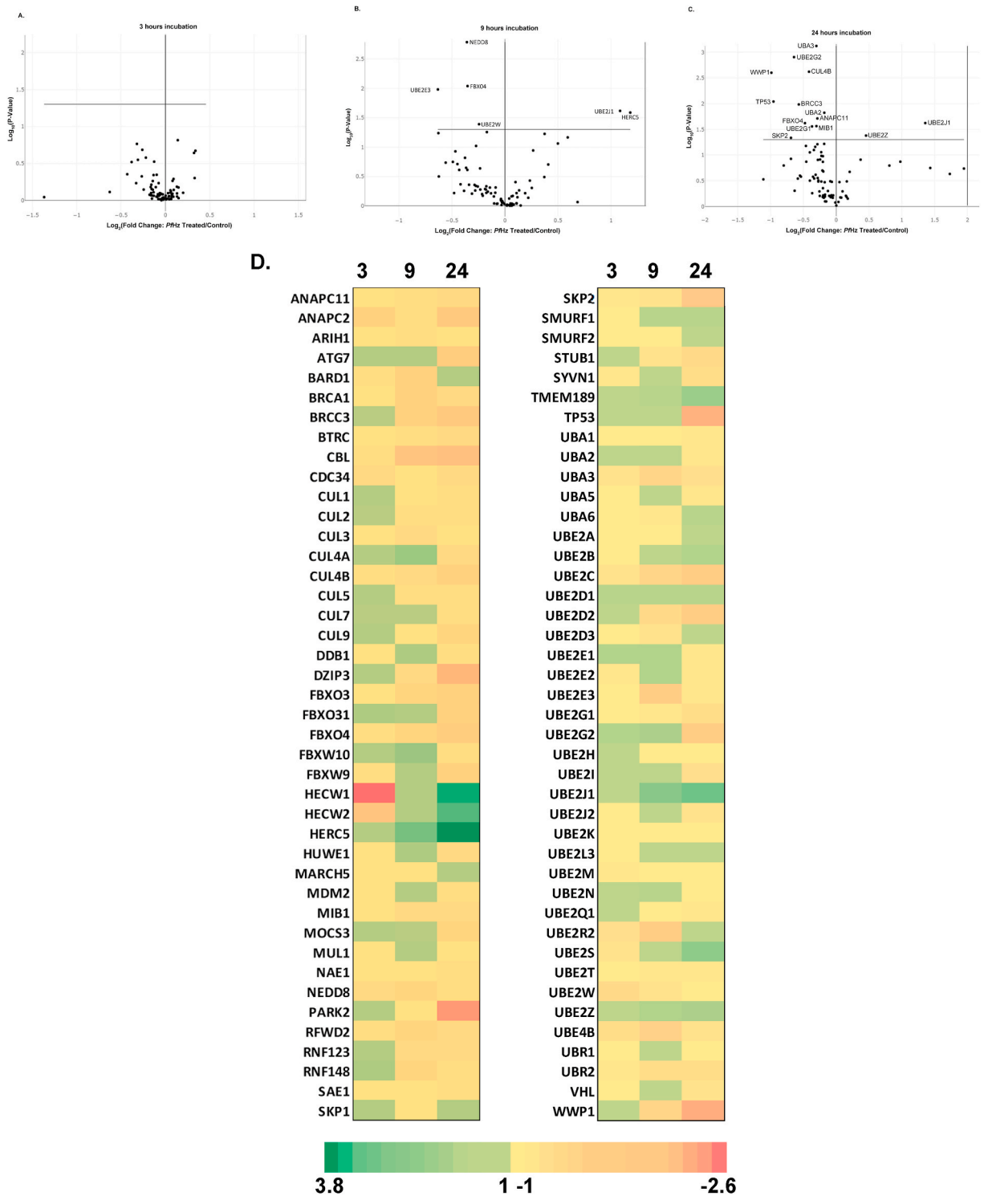

Fig. 2. Comparison of Ubiquitination gene expression levels between control and *Pf*Hz-treated PBMCs. Cells were isolated from malaria naïve healthy donors (n = 3). Peripheral blood mononuclear cells (PBMCs) were seeded in RPMI 1640 medium, and cultured at intervals of 3, 9 and 24 h in a humidified incubator set at 37°C in 5% CO_2 atmosphere. Gene expression profiles were measured using the Human Ubiquitination Pathway RT^2 Profiler PCR Array kit. Geometric mean was used as a normalization factor, and data was standardized using 5 housekeeping genes [Actin, beta (*ACTB*), Beta-2-microglobulin (*B2M*), Glyceraldehyde-3-phosphate dehydrogenase (*GAPDH*), Hypoxanthine phosphoribosyltransferase 1 (*HPRT1*) and Ribosomal protein, large, P0 (*RPLP0*)]. Data were analyzed by the $^{\Delta\Delta}C_T$ method ($2^{-\Delta\Delta C_T}$), using the RT^2 Profiler PCR Array GeneGlobe Data Analysis Center (https://geneglobe.qiagen.com/us/analyze). Fold regulation was set at 1.5, and $P \leq 0.050$ was considered statistically significant. A-C. Volcano Plot shows the Log_2 of the fold changes at 3 h (A), 9 h (B), and 24 h (C) post stimulation of the average gene expression on the x-axis versus their statistical significance on the y-axis. The center vertical line indicates unchanged gene expression, while the two outer vertical lines indicate the selected fold regulation threshold. D. Heat map showing the graphical and color-coded representation of fold regulation expression data between control (non-stimulated) and *Pf*Hz stimulated PBMCs at 3-, 9- and 24 h. The yellow color represents the average magnitude of gene expression. The brightest red represents the smallest value, and the brightest green represents the highest value. E. Cluster gram of non-supervised hierarchical clustering showing a heat map with dendrograms indicating co-regulated genes of the control (non-stimulated) and *Pf*Hz stimulated PBMCs at 3-, 9- and 24 h. Geometric mean was used as a normalization factor.

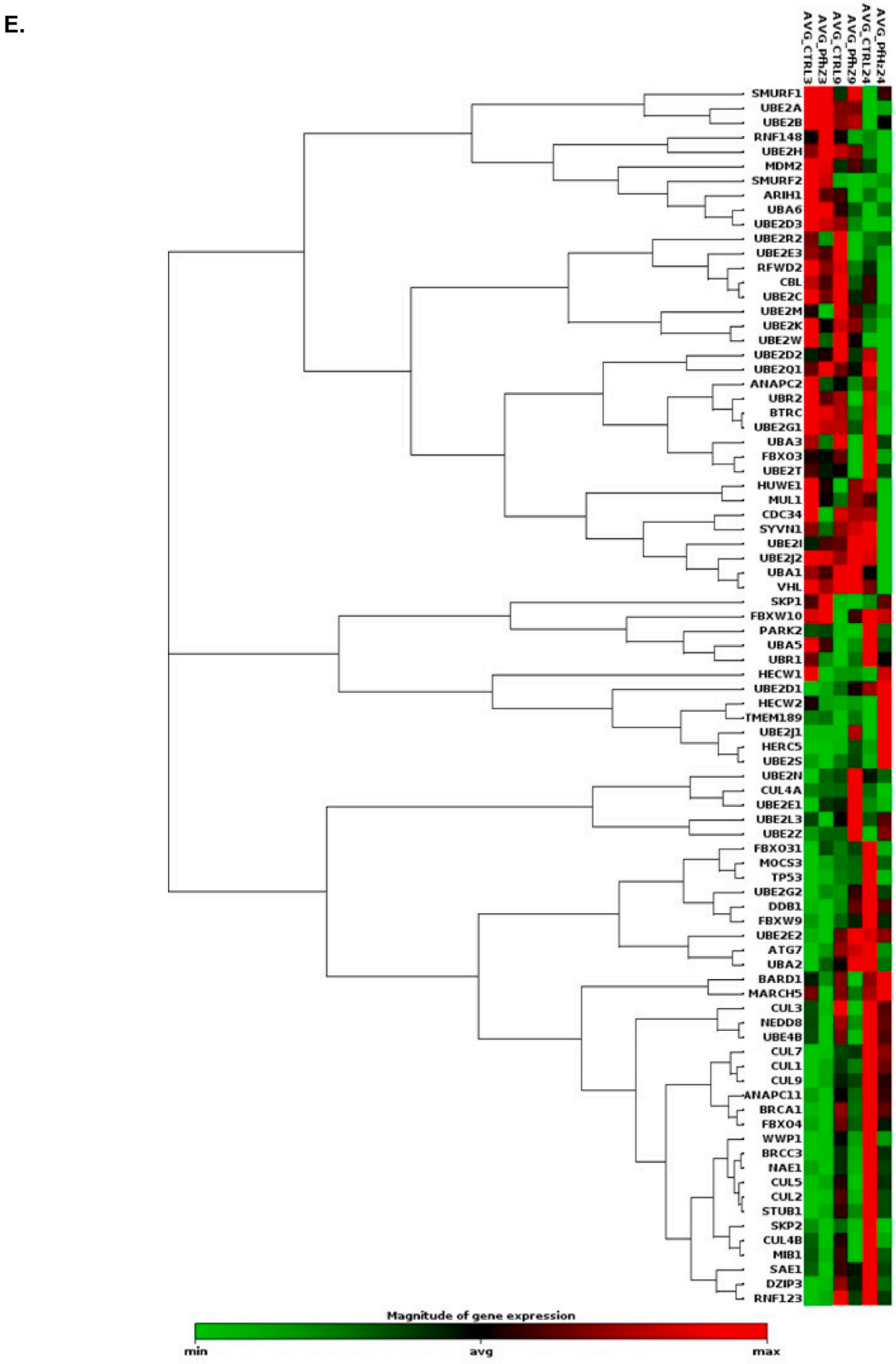

Fig. 2. (*continued*).

Ubiquitination mRNA transcript levels between Control (non-stimulated) and *Pf*Hz stimulated PBMCs.

Genes				2^(-Avg. (Delta(Ct))		Fold Change	Fold Regulation	*P*-value
Reference Sequence	Symbol	Description	Gene Name	Control Group	Stimulated Group	Stimulated Group		
9 h Incubation								
NM_012176	FBXO4	F-box protein 4	FBX4	0.011829	0.009266	0.78	−1.28	0.009
NM_016323	HERC5	Hect domain and RLD 5	CEB1/CEBP1	0.011166	0.025316	**2.27**	**2.27**	0.026
NM_006156	NEDD8	Neural precursor cell expressed, developmentally down-regulated 8	NEDD-8	0.092304	0.071985	0.78	−1.28	0.002
NM_006357	UBE2E3	Ubiquitin-conjugating enzyme E2E 3	UBCH9/UbcM2	0.049768	0.032114	**0.65**	**−1.55**	0.010
NM_016021	UBE2J1	Ubiquitin-conjugating enzyme E2, J1, U	CGI-76/HSPC153/HSPC205/ HSU93243/NCUBE-1/NCUBE1/ UBC6/UBC6E	0.033055	0.070131	**2.12**	**2.12**	0.024
NM_018299	UBE2W	Ubiquitin-conjugating enzyme E2W (putative)	UBC-16/UBC16	0.056314	0.047551	0.84	−1.18	0.041
24 h Incubation								
NM_001002244	ANAPC11	Anaphase promoting complex subunit 11	APC11/Apc11p/HSPC214	0.045042	0.036938	0.82	−1.22	0.019
NM_024332	BRCC3	BRCA1/BRCA2-containing complex, subunit 3	BRCC36/C6.1A/CXorf53	0.008227	0.005545	0.67	−1.48	0.010
NM_003588	CUL4B	Cullin 4B	CUL-4B/MRXHF2/MRXS15/ MRXSC/SFM2	0.034379	0.025813	0.75	−1.33	0.002
NM_012176	FBXO4	F-box protein 4	FBX4	0.014415	0.010367	0.72	−1.39	0.024
NM_020774	MIB1	Mindbomb homolog 1 (Drosophila)	DIP-1/DIP1/LVNC7/MIB/ZZANK2/ ZZZ6	0.019969	0.016213	0.81	−1.23	0.027
NM_005983	SKP2	S-phase kinase-associated protein 2 (p45)	FBL1/FBXL1/FLB1/p45	0.009278	0.005756	**0.62**	**−1.61**	0.046
NM_000546	TP53	Tumor protein p53	BCC7/LFS1/P53/TRP53	0.065982	0.034043	**0.52**	**−1.94**	0.009
NM_005499	UBA2	Ubiquitin-like modifier activating enzyme 2	ARX/HRIHFB2115/SAE2	0.058657	0.051748	0.88	−1.13	0.015
NM_003968	UBA3	Ubiquitin-like modifier activating enzyme 3	NAE2/UBE1C/hUBA3	0.048547	0.039395	0.81	−1.23	0.001
NM_003342	UBE2G1	Ubiquitin-conjugating enzyme E2G 1	E217K/UBC7/UBE2G	0.018536	0.014361	0.77	−1.29	0.028
NM_182688	UBE2G2	Ubiquitin-conjugating enzyme E2G 2	UBC7	0.018943	0.012139	**0.64**	**−1.56**	0.001
NM_016021	UBE2J1	Ubiquitin-conjugating enzyme E2, J1, U	CGI-76/HSPC153/HSPC205/ HSU93243/NCUBE-1/NCUBE1/ UBC6/UBC6E/Ubc6p	0.031618	0.080981	**2.56**	**2.56**	0.024
NM_023079	UBE2Z	Ubiquitin-conjugating enzyme E2Z	HOYS7/USE1	0.038841	0.053222	1.37	1.37	0.042
NM_007013	WWP1	WW domain containing E3 ubiquitin protein ligase 1	AIP5/Tiul1/hSDRP1	0.066533	0.033581	**0.50**	**−1.98**	0.002

Data presented as fold regulation of differentially expressed genes (n = 84) of the ubiquitination process. Cells were isolated from malaria naïve healthy US donors (n = 3). Peripheral blood mononuclear cells (PBMCs) were seeded in RPMI 1640 medium, and cultured at intervals of 3-, 9-, and 24 h in a humidified incubator set at 37°C in 5% CO_2 atmosphere. Gene expression profiles were measured using the Human Ubiquitination Pathway RT^2 Profiler PCR Array kit. Fold-Change ($2^{-\Delta\Delta}C_T$) represents the normalized gene expression ($2^{-\Delta}C_T$) in the *Pf*Hz-stimulated PBMCs divided the normalized gene expression ($2^{-\Delta}C_T$) in the control (non-stimulated) PBMCs. The data were normalized with 5 housekeeping genes [Actin, beta (*ACTB*), Beta-2-microglobulin (*B2M*), Glyceraldehyde-3-phosphate dehydrogenase (*GAPDH*), Hypoxanthine phosphoribosyltransferase 1 (*HPRT1*) and Ribosomal protein, large, P0 (*RPLPO*)]. Data were analyzed by the $^{\Delta\Delta}C_T$ method ($2^{-\Delta\Delta}C_T$), using the RT^2 Profiler PCR Array GeneGlobe Data Analysis Center (https://geneglobe.qiagen.com/us/analyze). *P*-values were calculated using the student's *t*-test of the triplicate raw C_T values. $P \leq 0.050$ was considered statistically significant.

regulation for 5 genes (Table 1). The gene coding for *UBE2J1* was up-regulated (fold-regulation = 2.56, $P = 0.024$) and showed an increase of expression that was higher than that observed after 9 h of treatment. There were 4 genes that were down-regulated at 24 h: the genes that code the S-phase kinase-associated protein 2 (*SKP2*; fold-regulation = −1.61, $P = 0.046$), Tumor protein p53 (*TP53*; fold-regulation = −1.94, $P = 0.009$), Ubiquitin-conjugating enzyme E2G 2 (*UBE2G2*; fold-regulation = −1.56, $P = 0.001$), and the WW domain containing E3 ubiquitin protein ligase 1 (*WWP1*; fold-regulation = −1.98, $P = 0.002$). All four of the genes that were suppressed at ≥1.5-fold regulation at 24 h did not show such down-regulation at the 9 h timepoint.

4. Discussion

Our recent studies in children from a *P. falciparum* holoendemic region of Kenya with either mild malarial anemia (Hb ≥ 9.0 g/dL, n = 23) or severe malaria anemia (Hb < 6.0 g/dL, n = 21) showed significant differential expression for genes involved in the human ubiquitination process [17]. To extend the findings, we analyzed the same panel of 84 key genes involved in the host ubiquitination process using an *in vitro* model for malaria [3,8,18,19,24]. Since we used a concentration of hemozoin (10 μg/mL) that parallels that present in children with severe malaria, results presented here can be interpreted in the context of severe disease [3,8,18]. Our previous studies and those of others illustrate that cultured PBMCs treated with physiological concentrations of *Pf*Hz are an excellent *in vitro* model for malaria since perturbations of cytokine, chemokine, and effector molecule transcripts and protein levels mimic those observed in children with severe malarial anemia [3,8,22,25,26]. Utilization of the *in vitro* model allowed us to capture rapid changes in the temporal dynamics of ubiquitination genes without the need for repeated blood collection over a short period of time, a practice that is not viable in children with severe malaria who suffer from markedly low hemoglobin levels. Since the time at which individuals become infected with malaria is variable and largely unknown upon

presentation at hospital when blood samples are collected, the *in vitro* model also allowed us to capture short-term changes in ubiquitination genes that cannot be achieved for natural infections. Thus, the experimental design enabled measurement of DEG for ubiquitination processes that are early in the infection phase versus those that would be observed during later disease progression for which the precise infection time is unattainable.

Stimulation of cultured PBMCs with *Pf*Hz for 3 h did not yield DEG for any of the 84 ubiquitination genes analyzed, indicating that the effects of hemozoin on ubiquitination are not immediate. These results parallel our previous data in which differential expression for innate immune response genes was not observed after 3 h of treatment with *Pf*Hz [19,24]. However, continued stimulation for 9 and 24 h resulted in significant DEG for 6 and 14 ubiquitination genes, respectively. The majority of significantly dysregulated genes at 9 h (4 of 6) and 24 h (12 of 14) were down-regulated, suggesting that phagocytosis of *Pf*Hz disrupts ubiquitination by potentially suppressing genes that may be required to maintain appropriate cellular functions during a stress response.

For the genes with significant differential regulation, those with a fold-regulation $\geq$1.5 at 9 h were *HERC5*, *UBE2J1*, and *UBE2E3*, while those at 24 h were *UBE2J1*, *SKP2*, *TP53*, *UBE2G2*, and *WWP1*. Previous studies have shown that *HERC5*, a ubiquitin ligase that conjugates interferon-stimulating gene 15, is up-regulated by pro-inflammatory cytokines [27,28]. Thus, up-regulation at 9 h is consistent with our findings showing that stimulation of PBMCs with *Pf*Hz during this timeframe induces the production of pro-inflammatory mediators [3,5,24]. The only gene in the panel that showed significant dysregulation at both 9 and 24 h was *UBE2J1*, an enzyme that catalyzes the covalent attachment of ubiquitin to other proteins and their degradation [29]. Since *UBE2J1* is essential for endoplasmic reticulum stress recovery and is rapidly degraded by the proteasome, sustained up-regulation of *UBE2J1* over 24 h suggests an ongoing cellular stress in response to *Pf*Hz [30]. Side-by-side clustering of *HERC5* and *UBE2J1* suggests that these two genes may be co-regulated. Genes that were down-regulated at a fold-regulation of $\geq$1.5 included *UBE2E3* at 9 h and *SKP2*, *TP53*, *UBE2G2*, and *WWP1* at 24 h. *UBE2E3* did not cluster with any of the other down-regulated genes. *SKP2* and *WWP1* formed a distal common regulation pattern, whereas side-by-side clustering of *TP53* and *UBE2G2* suggest strong co-regulation. Based on the roles these genes play in maintaining cellular homeostasis, it appears that their reduced expression following the phagocytosis of *Pf*Hz can elicit impairments in cellular proliferation, DNA repair, cell senescence, cell cycle arrest, apoptosis, degradation of immunoreceptors and proteins, transcription, and RNA splicing [31–34]. The dynamic temporal down- and up-regulation of the ubiquitination process genes shown here is consistent with results of other studies investigating various gene interaction models utilizing enrichment and network analysis [35]. The gene expression patterns at 9 h and 24 h are consistent with recovery to physiological levels. Absence of differential expression at 24 h after treatment with *Pf*Hz for the genes up-regulated (*HERC5*) or down-regulated (*NEDD8*, *UBE2E3* and *UBE2W*) at 9-h post treatment suggest recovery to normal expression levels.

In conclusion, results presented here reveal temporal expression of mRNA transcripts in ubiquitination process genes upon stimulation of PBMCs with physiological concentrations of *Pf*Hz. These results complement our recent studies in children with mild- and severe malaria showing DEG for ubiquitination processes. We propose that disruption in ubiquitination processes may be a previously unrecognized pathophysiological mechanism for severe malaria.

Statement

The study was approved by the Kenya Medical Research Institute Scientific and Ethics Review Unit, the University of New Mexico Institutional Review Board, and the Maseno University Ethics Review Committee. Informed consent was obtained for experimentation with human samples.

Financial support

The work was supported by National Institutes of Health (NIH) Research Grants R01AI130473 and R01AI51305 (DJP), NIH Fogarty International Center Grants K43TW011581 (SBA), D43TW05884 (DJP, SBA) and D43TW010543 (SBA, DJP), and Los Alamos National Laboratory, Laboratory Directed Research and Development Grant 20150090DR (BHM, DJP).

Declaration of interests

The authors declare that they have no known competing financial interests or personal relationships that could have appeared to influence the work reported in this paper.

Acknowledgements

The authors gratefully acknowledge the assistance of the University of New Mexico-Kenya team: Nicholas Otieno Ondiek, Anne A Ong'ondo, Chrispine Wasonga, Joan L A Ochieng, Rodney B Mongare, and Vincent Omanje.

References

[1] WHO, World Malaria Report 2020, World Health Organization, Geneva, 2020. World Health Organization, 2020.
[2] T. Nebl, M.J. De Veer, L. Schofield, Stimulation of innate immune responses by malarial glycosylphosphatidylinositol via pattern recognition receptors, Parasitology 130 (Suppl) (2005) S45–S62.
[3] G.A. Awandare, Y. Ouma, C. Ouma, T. Were, R. Otieno, C.C. Keller, G. C. Davenport, J.B. Hittner, J. Vulule, R. Ferrell, J.M. Ong'echa, D.J. Perkins, Role of monocyte-acquired hemozoin in suppression of macrophage migration inhibitory factor in children with severe malarial anemia, Infect. Immun. 75 (2007) 201–210.
[4] C. Casals-Pascual, O. Kai, J.O. Cheung, S. Williams, B. Lowe, M. Nyanoti, T. N. Williams, K. Maitland, M. Molyneux, C.R. Newton, N. Peshu, S.M. Watt, D. J. Roberts, Suppression of erythropoiesis in malarial anemia is associated with hemozoin in vitro and in vivo, Blood 108 (2006) 2569–2577.
[5] D.J. Perkins, T. Were, G.C. Davenport, P. Kempaiah, J.B. Hittner, J.M. Ong'echa, Severe malarial anemia: innate immunity and pathogenesis, Int. J. Biol. Sci. 7 (2011) 1427–1442.
[6] P.H. Nguyen, N. Day, T.D. Pram, D.J. Ferguson, N.J. White, Intraleucocytic malaria pigment and prognosis in severe malaria, Trans. R. Soc. Trop. Med. Hyg. 89 (1995) 200–204.
[7] P.G. Kremsner, C. Valim, M.A. Missinou, C. Olola, S. Krishna, S. Issifou, M. Kombila, L. Bwanaisa, S. Mithwani, C.R. Newton, T. Agbenyega, M. Pinder, K. Bojang, D. Wypij, T. Taylor, Prognostic value of circulating pigmented cells in African children with malaria, J. Infect. Dis. 199 (2009) 142–150.
[8] T. Were, G.C. Davenport, E.O. Yamo, J.B. Hittner, G.A. Awandare, M.F. Otieno, C. Ouma, A.S. Orago, J.M. Vulule, J.M. Ong'echa, D.J. Perkins, Naturally acquired hemozoin by monocytes promotes suppression of RANTES in children with malarial anemia through an IL-10-dependent mechanism, Microb. Infect. 11 (2009) 811–819.
[9] A. Brehm, E. Kruger, Dysfunction in protein clearance by the proteasome: impact on autoinflammatory diseases, Semin. Immunopathol. 37 (2015) 323–333.
[10] G. Cetin, S. Klafack, M. Studencka-Turski, E. Kruger, F. Ebstein, The ubiquitin-proteasome system in immune cells, Biomolecules 11 (2021).
[11] A.L. Haas, T.J. Siepmann, Pathways of ubiquitin conjugation, Faseb. J. 11 (1997) 1257–1268.
[12] C.M. Pickart, M.J. Eddins, Ubiquitin: structures, functions, mechanisms, Biochim. Biophys. Acta 1695 (2004) 55–72.
[13] C.M. Pickart, Mechanisms underlying ubiquitination, Annu. Rev. Biochem. 70 (2001) 503–533.
[14] C.E. Berndsen, C. Wolberger, New insights into ubiquitin E3 ligase mechanism, Nat. Struct. Mol. Biol. 21 (2014) 301–307.
[15] W. Li, M.H. Bengtson, A. Ulbrich, A. Matsuda, V.A. Reddy, A. Orth, S.K. Chanda, S. Batalov, C.A. Joazeiro, Genome-wide and functional annotation of human E3 ubiquitin ligases identifies MULAN, a mitochondrial E3 that regulates the organelle's dynamics and signaling, PLoS One 3 (2008), e1487.
[16] A. Warnatsch, T. Bergann, E. Kruger, Oxidation matters: the ubiquitin proteasome system connects innate immune mechanisms with MHC class I antigen presentation, Mol. Immunol. 55 (2013) 106–109.
[17] S.B. Anyona, E. Raballah, Q. Cheng, I. Hurwitz, C. Ndege, E. Munde, W. Otieno, P. D. Seidenberg, K.A. Schneider, C.G. Lambert, B.H. McMahon, C. Ouma, D.

J. Perkins, Differential gene expression in host ubiquitination processes in childhood malarial anemia, Front. Genet. 12 (2021) 764759.
[18] C.C. Keller, P.G. Kremsner, J.B. Hittner, M.A. Misukonis, J.B. Weinberg, D. J. Perkins, Elevated nitric oxide production in children with malarial anemia: hemozoin-induced nitric oxide synthase type 2 transcripts and nitric oxide in blood mononuclear cells, Infect. Immun. 72 (2004) 4868–4873.
[19] P. Kempaiah, K. Dokladny, Z. Karim, E. Raballah, J.M. Ong'echa, P.L. Moseley, D. J. Perkins, Reduced Hsp70 and glutamine in pediatric severe malaria anemia: role of hemozoin in suppressing Hsp70 and NF-kappaB activation, Mol. Med. 22 (2016) 570–584.
[20] W. Trager, J.B. Jensen, Human malaria parasites in continuous culture, Science 193 (1976) 673–675.
[21] C. Lambros, J.P. Vanderberg, Synchronization of Plasmodium falciparum erythrocytic stages in culture, J. Parasitol. 65 (1979) 418–420.
[22] C.C. Keller, J.B. Hittner, B.K. Nti, J.B. Weinberg, P.G. Kremsner, D.J. Perkins, Reduced peripheral PGE2 biosynthesis in Plasmodium falciparum malaria occurs through hemozoin-induced suppression of blood mononuclear cell cyclooxygenase-2 gene expression via an interleukin-10-independent mechanism, Mol. Med. 10 (2004) 45–54.
[23] K.J. Livak, T.D. Schmittgen, Analysis of relative gene expression data using real-time quantitative PCR and the 2(-Delta Delta C(T)) Method, Methods 25 (2001) 402–408.
[24] A.O. Achieng, B. Guyah, Q. Cheng, J.M. Ong'echa, C. Ouma, C.G. Lambert, D. J. Perkins, Molecular basis of reduced LAIR1 expression in childhood severe malarial anaemia: implications for leukocyte inhibitory signalling, EBioMedicine 45 (2019) 278–289.
[25] G. Giribaldi, M. Prato, D. Ulliers, V. Gallo, E. Schwarzer, O.B. Akide-Ndunge, E. Valente, S. Saviozzi, R.A. Calogero, P. Arese, Involvement of inflammatory chemokines in survival of human monocytes fed with malarial pigment, Infect. Immun. 78 (2010) 4912–4921.
[26] M.T. Shio, F.A. Kassa, M.J. Bellemare, M. Olivier, Innate inflammatory response to the malarial pigment hemozoin, Microb. Infect. 12 (2010) 889–899.
[27] A. Dastur, S. Beaudenon, M. Kelley, R.M. Krug, J.M. Huibregtse, Herc5, an interferon-induced HECT E3 enzyme, is required for conjugation of ISG15 in human cells, J. Biol. Chem. 281 (2006) 4334–4338.
[28] R. Kroismayr, U. Baranyi, C. Stehlik, A. Dorfleutner, B.R. Binder, J. Lipp, HERC5, a HECT E3 ubiquitin ligase tightly regulated in LPS activated endothelial cells, J. Cell Sci. 117 (2004) 4749–4756.
[29] U. Lenk, H. Yu, J. Walter, M.S. Gelman, E. Hartmann, R.R. Kopito, T. Sommer, A role for mammalian Ubc6 homologues in ER-associated protein degradation, J. Cell Sci. 115 (2002) 3007–3014.
[30] M. Elangovan, H.K. Chong, J.H. Park, E.J. Yeo, Y.J. Yoo, The role of ubiquitin-conjugating enzyme Ube2j1 phosphorylation and its degradation by proteasome during endoplasmic stress recovery, J. Cell Commun. Signal 11 (2017) 265–273.
[31] K.S. Plafker, K. Zyla, W. Berry, S.M. Plafker, Loss of the ubiquitin conjugating enzyme UBE2E3 induces cellular senescence, Redox Biol. 17 (2018) 411–422.
[32] J. Wu, S.W. Lee, X. Zhang, F. Han, S.Y. Kwan, X. Yuan, W.L. Yang, Y.S. Jeong, A. H. Rezaeian, Y. Gao, Y.X. Zeng, H.K. Lin, Foxo3a transcription factor is a negative regulator of Skp2 and Skp2 SCF complex, Oncogene 32 (2013) 78–85.
[33] E. Toufektchan, F. Toledo, The guardian of the genome revisited: p53 downregulates genes required for telomere maintenance, DNA repair, and centromere structure, Cancers 10 (2018).
[34] Y. Yang, B. Liao, S. Wang, B. Yan, Y. Jin, H.B. Shu, Y.Y. Wang, E3 ligase WWP2 negatively regulates TLR3-mediated innate immune response by targeting TRIF for ubiquitination and degradation, Proc. Natl. Acad. Sci. U. S. A. 110 (2013) 5115–5120.
[35] Y. Liu, M. Koyuturk, J.S. Barnholtz-Sloan, M.R. Chance, Gene interaction enrichment and network analysis to identify dysregulated pathways and their interactions in complex diseases, BMC Syst. Biol. 6 (2012) 65.